Kinetic and safety parameters analysis for 1,1,-di-(tert-butylperoxy)-3,3,5-trimethylcyclohexane in isothermal and non-isothermal conditions

Jo-Ming Tseng [a,*], Chun-Ping Lin [b], Sheng-Tien Huang [a], Johnson Hsu [c]

[a] Institute of Safety and Disaster Prevention Technology, Central Taiwan University of Science and Technology, 666, Buzih Rd., Beitun District, Taichung 40601, Taiwan, ROC
[b] Department of Health and Nutrition Biotechnology, Asia University, 500, Lioufeng Rd., Wufeng, Taichung 41354, Taiwan, ROC
[c] TA Instruments-Waters LLC, 23, Sec. 1, Chang-an East Road, Taipei 104, Taiwan, ROC

ARTICLE INFO

ABSTRACT

Over the past 30 years, the field of thermal analysis of organic peroxides has become an important issue in chemical engineering departments, safety departments, and in companies working with polymerization, petrifaction process, and so on. The contributions of thermal analysis to the evaluation and prediction of the runaway reactions have been important for decreasing or preventing a hazard, such as fire or explosion accident. This study was carried out using differential scanning calorimetry (DSC) to evaluate the kinetic and safety parameters in isothermal and non-isothermal conditions, for instance, temperature of no return (T_{NR}), self accelerating decomposition temperature (SADT), time to maximum rate (TMR), activation energy (E_a), frequency factor (A), reaction order (n), and reaction heat (ΔH), in terms of the hazardous material of 1,1,-di-(tert-butylperoxy)-3,3,5-trimethylcyclohexane (TMCH) 88 mass%. On the basis of this study, we demonstrated that TMCH 88 mass% must be well controlled in the manufacturing process due to the unstable structure of O–O, which releases a great quantity of heat, higher than 1300 J/g under decomposition. Results of this study could contribute to the relevant plants adopting TMCH 88 mass% in a process, in order to prevent a fire or explosion accident from happening.

© 2011 Elsevier B.V. All rights reserved.

1. Introduction

Runaway reactions [1,2] that induce fire or explosion accidents are familiar throughout the world, but how to prevent them is still a troublesome question in many countries. 1,1,-Di-(tert-butylperoxy)-3,3,5-trimethylcyclohexane (TMCH) 88 mass% has been employed as initiator and cross linker in the process of polymerization for a long time. Based on experimental results, TMCH could cause an explosive hazard if the process is out of control. When the heat release rate exceeds the heat removal rate, surplus heat could increase the temperature for a topic material. If the reaction temperature is increased rapidly with loss of control, a runaway reaction will be triggered in the next stage. Different types of phenomena have the potential to cause a runaway reaction in a reactor, which could result from difficulty in containing the accumulated reactant, wrong dosing, improper use of the catalytic agent, inappropriate operating in process, cooling system failure, external fire, external force effect, or stir failure. All these could arise from the reaction temperature increasing unusually and loss of control; afterwards, accidents are triggered, such as fires, explosions, toxic releases, and so on [3].

Heat accumulation plays an important role in runaway reactions. If the temperature is well controlled below the maximum permitted temperature during a process, a runaway reaction can be prevented easily. Therefore, a thermal curve is an efficient and reliable method adopted to design various protective measures, such as cooling system, blowdown tank, and even the emergency response plan. According to the previous database of accidents, organic peroxides are one of the main materials to form accidents [4], especially fire or explosion, due to the unstable structure of O–O, such as methyl ethyl ketone peroxide 15 mass% (405 J/g for second peak) [3], tert-butyl peroxybenzoate 98 mass% (1150 J/g) [5], cumene hydroperoxide 93 mass% (1399 J/g) [6], etc. As for the main grounds of runaway reactions, related staff often has insufficient knowledge with regard to unstable reactants [7–9], intermediate products, contaminants, so that the heat release in the start stage of decomposition cannot be detected immediately. A badly designed stirrer can easily affect the process conditions due to the poor mixing. Other causes are bad design of temperature detection in the reactor, faulty dosing rate, bad design of safety valve for emission volume, and incorrect operations. Safe ways to deal with upset situations are prediction,

prevention, and protection hazard, in terms of runaway reactions.

In this study, TMCH 88 mass% was evaluated for its thermal reactivity and runaway behavior using thermal analysis techniques. DSC was used to analyze the characterization of the temperature and heat power profiles of the TMCH 88 mass% reaction. Isothermal and non-isothermal conditions [10,11] were applied to analyze the effect of decomposition behavior during a runaway scenario. At the same time, theoretical evaluation was conducted to calculate kinetic and safety parameters to explain the experimental results and also to compare with other organic peroxides. This study indicated that TMCH 88 mass% has explosive characteristics under decomposition; therefore, the temperature control system must be well designed for decreasing the degree of hazard in the process stage.

2. Experimental setup

2.1. 1,1,-Di-(tert-butylperoxy)-3,3,5-trimethylcyclohexane (TMCH)

TMCH 88 mass%, which was purchased directly from ACE Chemical Corp in Taiwan, dibutyl phthalate (DBP) was used as dilution for compounding TMCH 22 and 44 mass% and stored in a refrigerator at 4 °C. Experiments were carried out by five types of heating rates of 1, 2, 4, 6, and 10 °C/min and four isothermal conditions of 115, 120, 125, and 130 °C. Structure of TMCH 88 mass% was as follows:
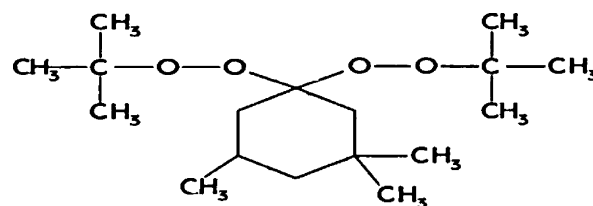
2.2. Well-known thermoanalytical technique property

Temperature-programmed screening experiments were performed with DSC (TA Q20). The test cell was used to carry out the experiment for withstanding relatively high pressure to approximately 10 MPa. ASTM E698 was used to obtain thermal curves for calculating kinetic parameters. For better thermal equilibrium, the heating rate chosen for the temperature-programmed ramp was not to exceed 10 °C/min. The range of temperature rise was chosen from 30 to 300 °C for each experiment. DSC is extensively employed to detect the temperature change between the sample and reference. We put the sample and the reference into the furnace heater to reach the temperature under investigation; a thermocouple was used to detect the temperature change (ΔT) between the sample and the reference. When the temperature reached a change-point, such as crystallization, boiling point, melting point, or induced thermal decomposition in the test cell, the environment was triggered to an unbalanced temperature between the sample and the reference, and then the heat-flow could be detected immediately for viewing on thermal curves.

3. Results and discussion

3.1. Kinetic evaluation

Three kinetic models were employed to evaluate the kinetic parameters for TMCH 88 mass%. The kinetic analyses of the exothermic peaks were conducted by five heating rates of 1, 2, 4, 6, and 8 °C/min and four isothermal conditions of 115, 120, 125, and 130 °C, shown in Tables 1–4 and Figs. 1–16, based on the Arrhenius [12], Kissinger [13], and Ozawa [14] equations. The performance of the E_a value depends on the variable of temperature point; therefore, the experimental procedure must proceed cautiously to reduce the errors made in experiment. In Table 1, we obtained an E_a about 122–140 kJ/mol in different heating rates by Arrhenius equation, and both of the equation methods of Kissinger [13] and Ozawa [14] were 134.08 and 134.05 kJ/mol, separately with higher R value of 0.99920 and 0.99927. It indicated that TMCH 88 mass% was a sensitive material due to its unstable structure of O–O, which can be seen in Figs. 1–6. Fig. 1 displays the decomposition reactions of TMCH 88 mass% in five types of heating rates. Three types of concentrations of TMCH 88, 44, and 22 mass% were carried out by heating rate of 4 °C/min in non-isothermal condition as shown

Table 1
Results of thermokinetic parameters for TMCH 88 mass% with heating rates of 1, 2, 4, 6, and 8 °C/min.

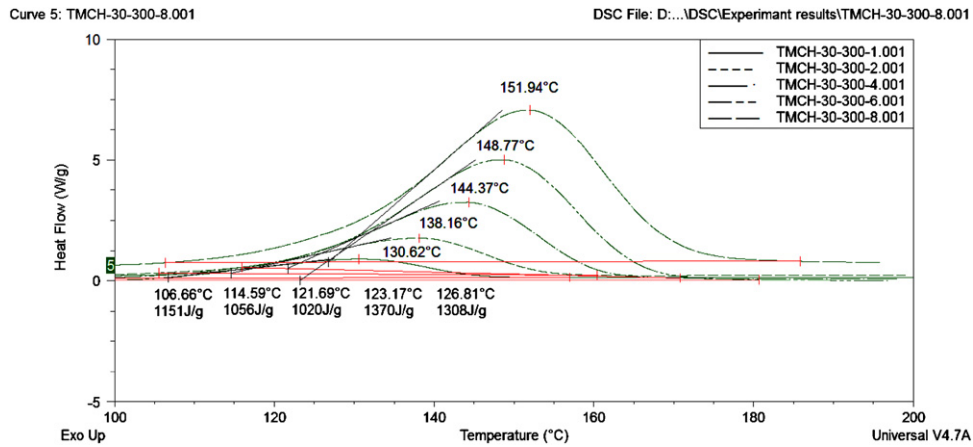| Sample	TMCH 88 mass%				
Heating rate (°C/min)	1	2	4	6	8
Sample mass (mg)	2.9	2.9	3.0	3.0	3.1
Onset temperature, T_o (°C)	106	114	121	123	126
Peak of Temperature, T_p (°C)	130	138	144	148	151
Frequency factor, A (ln 1/s)	30.5	35.8	33.5	35.5	30.1
Activation energy, E_a (kJ/mol)	124.3	141.6	133.9	140.8	122.7
Reaction order (n)	0.8	1.0	0.9	1.0	0.9
Reaction heat, ΔH (kJ/kg)	1151	1056	1020	1370	1308

Fig. 1. Thermal analysis of TMCH 88 mass% by DSC in non-isothermal conditions of 1, 2, 4, 6, and 8 °C/min.
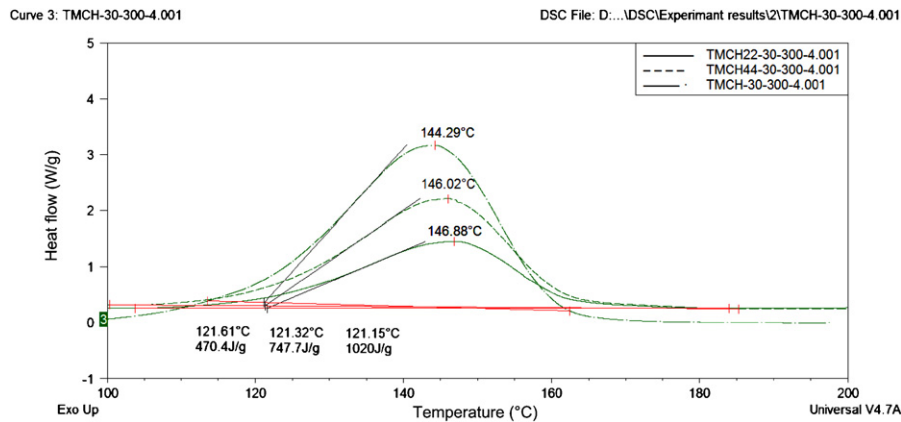

Fig. 2. Three types of concentrations of TMCH 88, 44, and 22 mass% tested by heating rate of 4 °C/min in non-isothermal conditions.

in Fig. 2 and Table 2. Both of the kinetic parameters of E_a and A were similar at about 162.9–163.2 kJ/mol and 41.8–42.1 ln 1/s, separately in lower concentrations of TMCH 22 and 44 mass%; while increasing the concentration to 88 mass%, the E_a and A were lower to 133.9 kJ/mol and 33.5 ln 1/s. It demonstrated that the higher con-

centration had increased the potential hazard, in terms of TMCH, due to its unstable structure of O–O. ΔH of TMCH 88, 44, and 22 mass% were ca. 1020, 747, and 470 kJ/kg. Fig. 3 is a plot of the natural logarithm of the various heating rates of 1, 2, 4, 6, and 8 °C/min versus the peak temperature $(1000/T_p(K))$, which provides
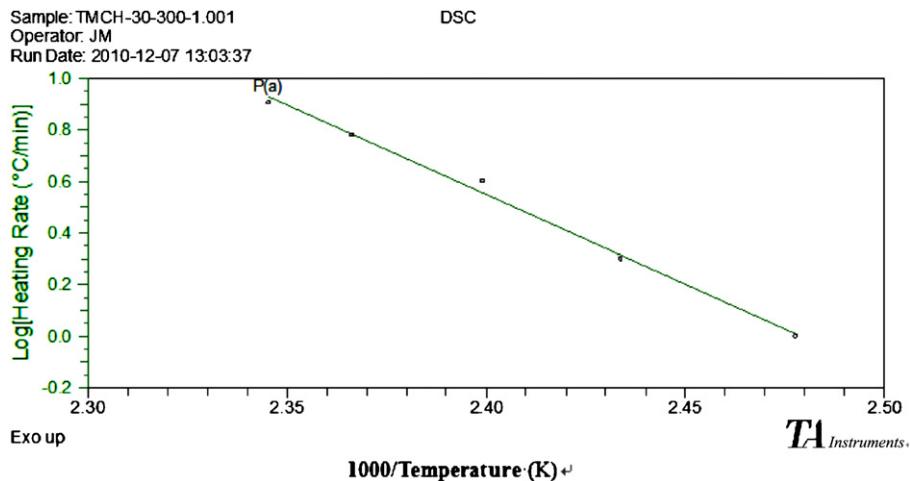

Fig. 3. Heating rate vs. $F[p(x)]$ of TMCH 88 mass% in non-isothermal conditions of 1, 2, 4, 6, and 8 °C/min.
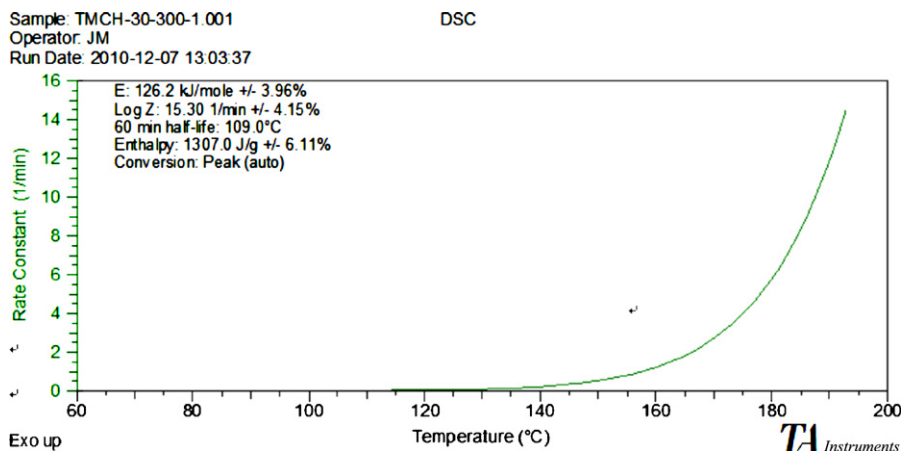
Sample: TMCH-30-300-1.001   DSC
Operator: JM
Run Date: 2010-12-07 13:03:37

E: 126.2 kJ/mole +/- 3.96%
Log Z: 15.30 1/min +/- 4.15%
60 min half-life: 109.0°C
Enthalpy: 1307.0 J/g +/- 6.11%
Conversion: Peak (auto)

Exo up

Fig. 4. Rate constant vs. temperature of TMCH 88 mass% in non-isothermal conditions.

Sample: TMCH-30-300-1.001   DSC
Operator: JM
Run Date: 2010-12-07 13:03:37

E: 126.2 kJ/mole +/- 3.96%
Log Z: 15.30 1/min +/- 4.15%
60 min half-life: 109.0°C
Enthalpy: 1307.0 J/g +/- 6.11%
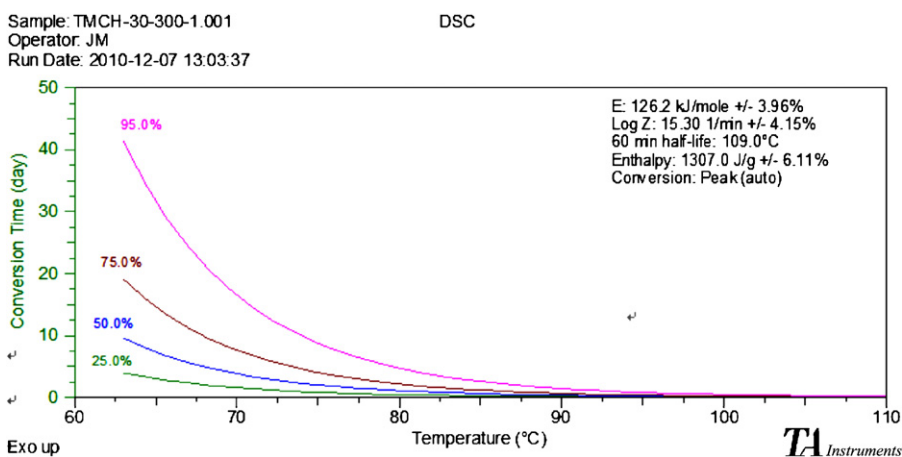Conversion: Peak (auto)

Exo up

Fig. 5. Conversion time vs. temperature of TMCH 88 mass% in non-isothermal conditions.

the information necessary to calculate the E_a, pre-exponential factor (A), reaction rate constant (k), and half-life, here assuming a first-order condition. Fig. 4 shows that A was obtained after E_a was by Fig. 3, and then $k = Ae[-E_a/RT]$ vs. temperature for TMCH 88 mass% in non-isothermal conditions. E_a and A were zoned into $d\alpha/dt = Ae[-E_a/RT](1-\alpha)$; afterward, time of conversion rate (α)

with 25%, 50%, 75%, and 95% in different reaction temperatures was drawn for TMCH 88 mass% in non-isothermal conditions, shown in Fig. 5. Fig. 6 indicates the time for α of 50% in different temperatures, for which so-called half-life, half-life vs. temperature of TMCH 88 mass% in non-isothermal conditions was obtained. Figs. 7 and 8 are the experimental results in isothermal conditions.

Sample: TMCH-30-300-1.001   DSC
Operator: JM
Run Date: 2010-12-07 13:03:37

E: 126.2 kJ/mole +/- 3.96%
Log Z: 15.30 1/min +/- 4.15%
60 min half-life: 109.0°C
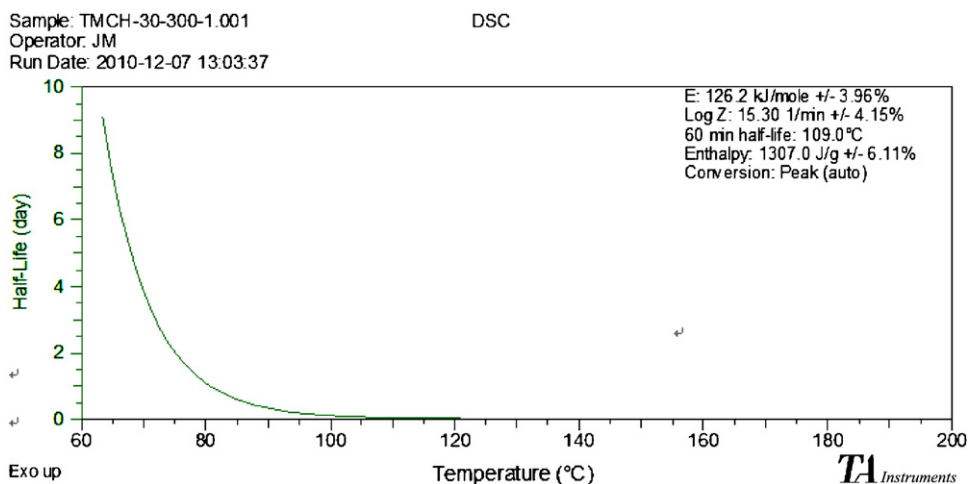Enthalpy: 1307.0 J/g +/- 6.11%
Conversion: Peak (auto)

Exo up

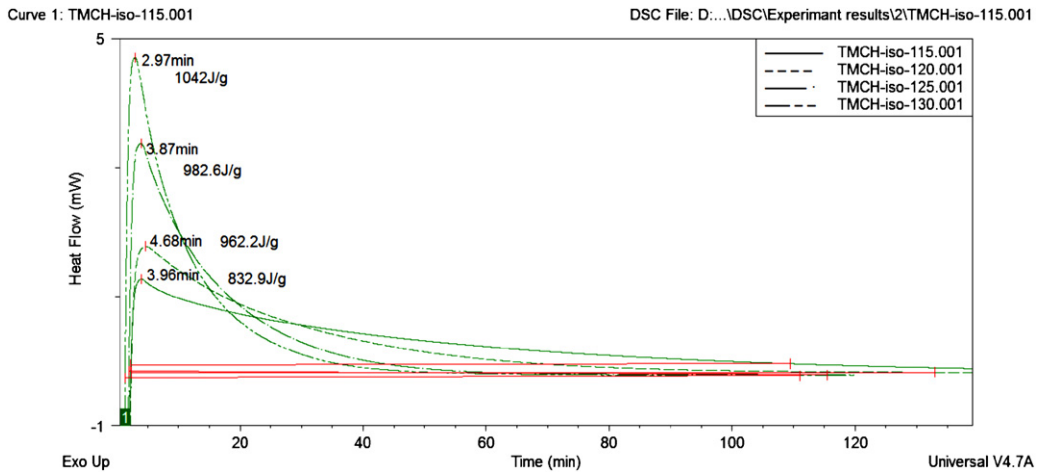**Fig. 6.** Half-life vs. temperature of TMCH 88 mass% in non-isothermal conditions.

Fig. 7. Thermal analysis of TMCH 88 mass% in isothermal conditions of 115, 120, 125, and 130 °C by DSC.
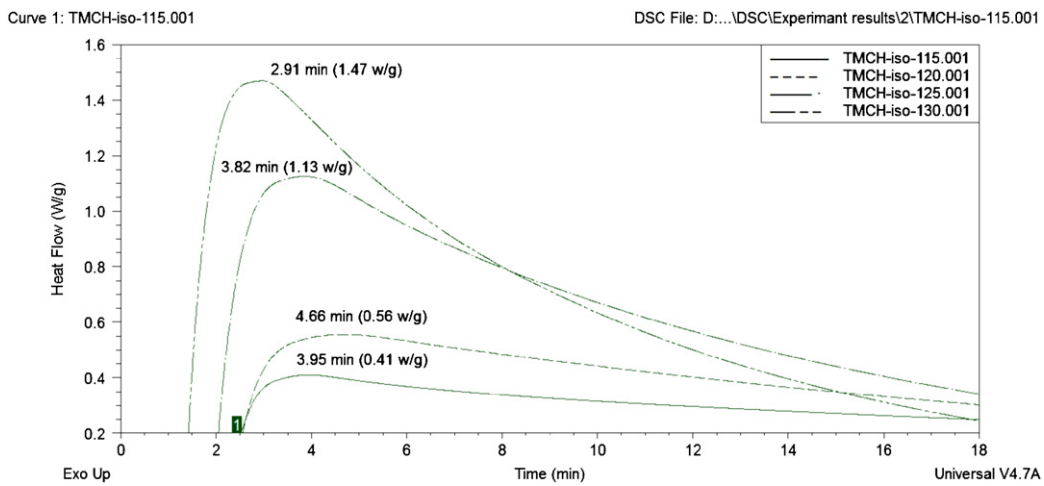

Fig. 8. TMR of TMCH 88 mass% in isothermal conditions of 115, 120, 125, and 130 °C.

Fig. 9 obtained the k by isothermal reaction data in 115 °C described of $\log[dC/dT]$ vs. $\log[1 - C]$; n was determined by the slope. Fig. 10 obtained the k by isothermal reaction data in 120 °C described of $\log[dC/dT]$ vs. $\log[1 - C]$, n was determined by the slope. Fig. 11 obtained the k by isothermal reaction data in 125 °C described of $\log[dC/dT]$ vs. $\log[1 - C]$; n was determined by the slope. Fig. 12 obtained the k by isothermal reaction data in 130 °C described of $\log[dC/dT]$ vs. $\log[1 - C]$; n again was gotten by slope. Fig. 13 was formed by four isothermal reaction data of 115 °C, 120 °C, 125 °C, and 130 °C for quantitative value optimization in $(1/k)(d\alpha/dt)$ vs. α;

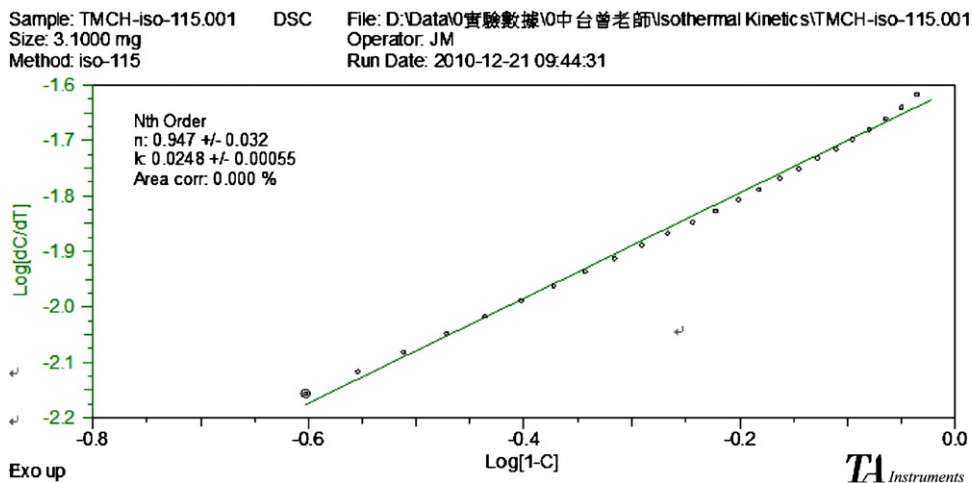**Fig. 9.** $\log[dC/dT]$ vs. $\log[1 - C]$ of TMCH 88 mass% in isothermal condition of 115 °C.
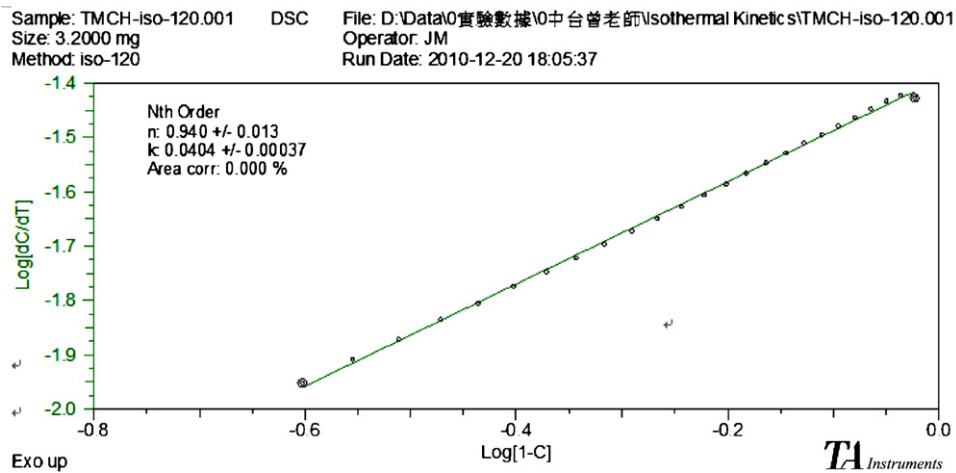
Fig. 10. Log[dC/dT] vs. log[$1 - C$] of TMCH 88 mass% in isothermal condition of 120 °C.

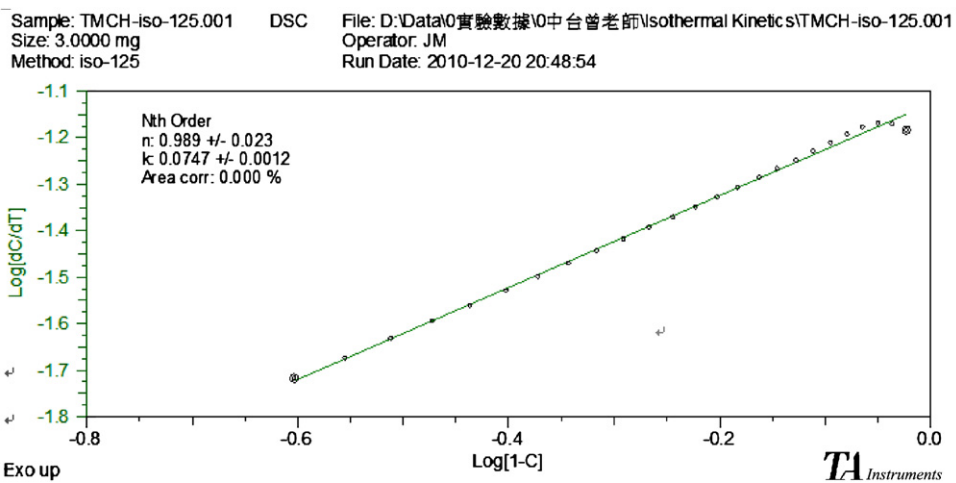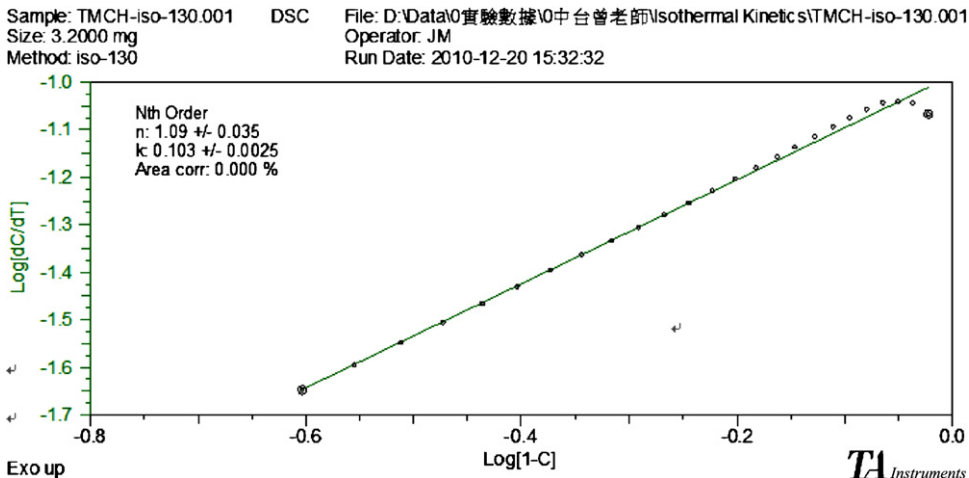**Fig. 11.** Log[dC/dT] vs. log[$1 - C$] of TMCH 88 mass% in isothermal condition of 125 °C.

Fig. 12. Log[dC/dT] vs. log[$1 - C$] of TMCH 88 mass% in isothermal condition of 130 °C.
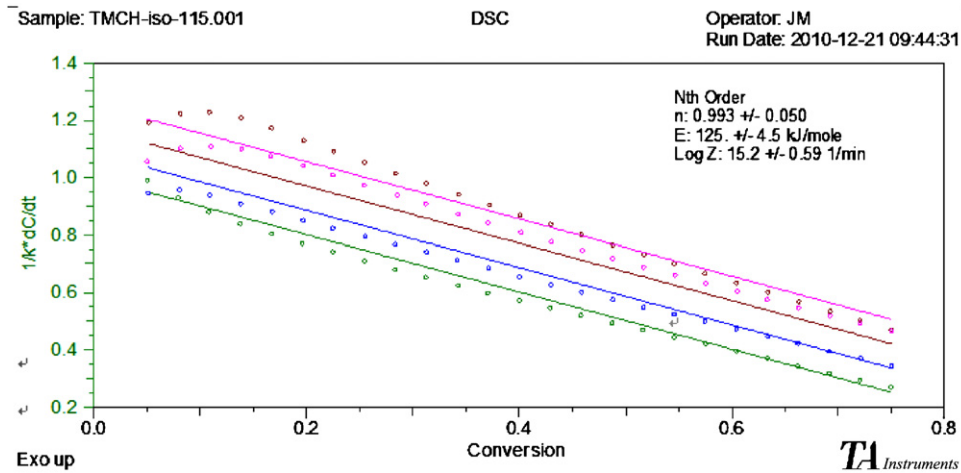
Fig. 13. $1/K^*dC/dT$ vs. conversion of TMCH 88 mass% in isothermal conditions.

Table 2
Results of thermokinetic parameters for TMCH 44 and 22 mass% with heating rate of 4 °C/min.

TMCH	22 mass%	44 mass%
Sample mass (mg)	2.9	2.9
Onset temperature, T_o (°C)	121	121
Peak of temperature, T_p (°C)	146	146
Frequency factor, A (ln $1/s$)	41.8	42.1
Activation energy, E_a (kJ/mol)	162.9	163.2
Reaction order (n)	1.2	1.1
Reaction heat, ΔH (kJ/kg)	470.4	747.7

Table 3
Calculation of E_a for TMCH 88 mass% with heating rates of 1, 2, 4, 6, and 8 °C/min by Kissinger and Ozawa equations.

Kinetic model	E_a (kJ/mol)	R
Kissinger equation	134.08	0.99920
Ozawa equation	134.05	0.99927

therefore, the optimums of n, A, and E_a were obtained in terms of TMCH 88 mass% in isothermal conditions. Kinetic parameters of n, A, and E_a were created according to the results of numerical analysis by Fig. 13; therefore, specific time of α in 25%, 50%, 75%, 95% was predictable in different reaction temperatures, illustrated in Fig. 14.

Table 4
ΔH, TMR, E_a, and n of TMCH 88 mass% in isothermal conditions of 115, 120, 125, and 130 °C.

Sample	TMCH 88 mass%			
Isothermal conditions (°C)	115	120	125	130
ΔH (J/g)	833	962	983	1042
TMR (min)	3.95	4.66	3.82	2.91
E_a (kJ/mol) by ln Q vs. T			118	
E_a (kJ/mol) by $1/K^*dC/dT$ vs. conversion			125	
n			0.993	

3.1.1. Arrhenius equation

Based on the Arrhenius equation [12],

$$-r_A = \frac{-dC_A}{dt} = kC_A^n = A \, \exp\left(\frac{-E_a}{RT}\right) C_A^n \tag{1}$$

where r_A is the reaction rate; C_A is the sample concentration; k is the reaction rate constant; n is the reaction order; A is the pre-exponential factor; E_a is the activation energy; T is the absolute temperature; R is the gas constant.
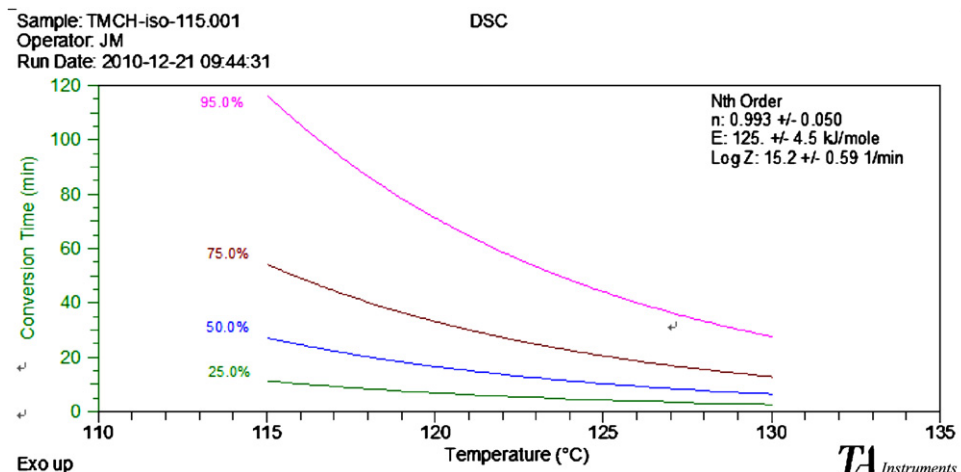
$$C_{A_0} = \frac{\rho}{M} \tag{2}$$

Fig. 14. Conversion time vs. temperature of TMCH 88 mass% in isothermal conditions.

Parameter	Value	Error
A	42.51975	4.65148
B	-14177.02035	1839.10915

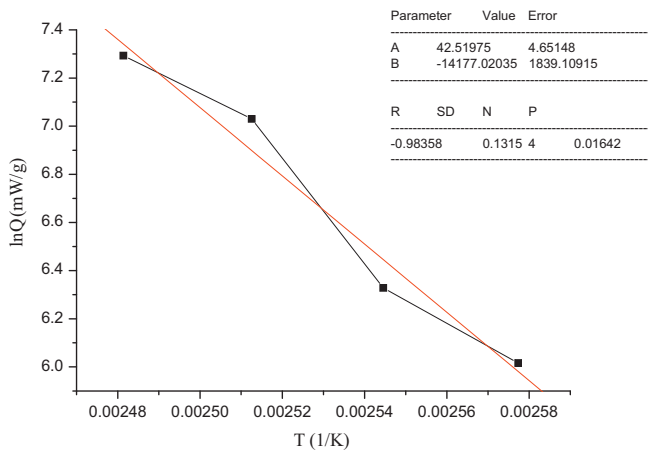| R	SD	N	P
-0.98358	0.1315	4	0.01642

Fig. 15. E_a calculation of TMCH 88 mass% in isothermal conditions of 115, 120, 125, and 130 °C.

where ρ is the sample density; M is the molecular weight; and C_{A_0} is the concentration,

$$C_A = C_{A_0}(1 - \alpha) \tag{3}$$

3.1.2. E_a evaluation of isothermal conditions

This was based on the results of isothermal conditions for TMCH 88 mass%, which indicated that TMCH 88 mass% obeyed the nth order reaction at the high temperature conditions of 115, 120, 125, and 130 °C, shown in Figs. 7–16. According to the configurations of heat release, the maximum heat flows were obtained at about 0.41–1.47 W/g in the beginning of starting experiment at isothermal conditions after 2–4 min, shown in Fig. 8. Reaction rate is shown as the following equations:

$$R = -\frac{d[\text{TMCH}]}{dt} = k[\text{TMCH}]^m \tag{4}$$

$$\dot{Q} = \frac{dQ}{dt} = \Delta H \cdot \rho \cdot V \cdot A \cdot e^{-E_a/RT} \cdot [\text{TMCH}]^m \cdot (1 - \alpha)^m \tag{5}$$

$$\ln Q \alpha \ln k = \ln C - \frac{E_a}{RT} \tag{6}$$

Based on the above-mentioned model, E_a was about 118 kJ/mol, as demonstrated in Fig. 15.

$$\frac{d\alpha}{dt} = k(1 - \alpha)^n \tag{7}$$

$$\frac{d\alpha}{dt} = Ae^{-E_a/RT}(1 - \alpha)^n \tag{8}$$

$$\ln\left[\frac{d\alpha}{dt}\right] = \ln(A) - \frac{E_a}{RT} + n\ln[1 - \alpha] \tag{9}$$

Isothermal temperature (T_i) was selected, and then:

$$\ln\left[\frac{d\alpha}{dt}\right] = n\ln[1 - \alpha] + \ln(A) - \frac{E_a}{RT_i} \tag{10}$$

By $\ln[d\alpha/dt]$ vs. $\ln[1 - \alpha]$, n is obtained by slope; in the meantime, k is obtained under T_i.

Data was obtained in Eq. (11) after carrying out more than three isothermal reaction experiments,

$$\frac{1}{k}\frac{d\alpha}{dt} = (1 - \alpha)^n \tag{11}$$

N, A, and E_a were obtained by $(1/k)(d\alpha/dt)$ vs. α in various isothermal conditions for proceeding quantitative value optimization.
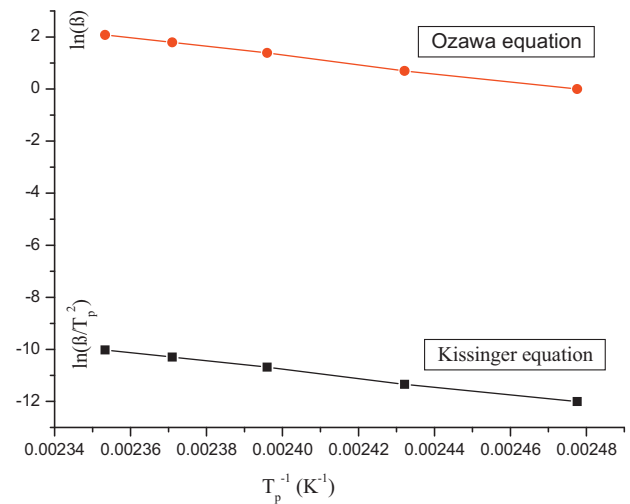

Fig. 16. Activation energy analysis graph for TMCH 88 mass% with different heating rates of 1, 2, 4, 6, and 8 °C/min by Kissinger and Ozawa equations.

3.1.3. Determination of E_a by Kissinger method

Kissinger method [13] is displayed as Eq. (12),

$$\ln\left(\frac{\beta}{T_P^2}\right) = \ln\frac{AR}{E} - \frac{E_a}{RT_P} \tag{12}$$

where β is the heating rate; T_p is the peak temperature; A is the pre-exponential factor; E_a is the activation energy; R is the gas constant. At the different heating rates, Kissinger's kinetic equation can be derived:

$$\ln\frac{\beta_1}{T_{P_1}^2} + \frac{E_a}{RT_{P_1}} = \ln\frac{\beta_2}{T_{P_2}^2} + \frac{E_a}{RT_{P_2}} = \ln\frac{\beta_3}{T_{P_3}^2} + \frac{E_a}{RT_{P_3}} = ..., \tag{13}$$

where β_1, β_2, and β_3 are the different heating rates; T_{P_1}, T_{P_2}, and T_{P_3} are the peak temperature of different heating rates. Results are displayed in Table 3 and Fig. 16.

3.1.4. Determination of E_a by Ozawa method

Ozawa method [14] is displayed as Eq. (18),

$$\frac{d\alpha}{dt} = Ae^{-E_a/RT}(1 - \alpha), \quad \text{for } n = 1 \tag{14}$$

$$\frac{dT}{dt}\frac{d\alpha}{dt} = Ae^{-E_a/RT}(1 - \alpha) \tag{15}$$

In which, $\beta = dT/dt$ (heating rate)

$$\ln\beta + \ln\left(\frac{d\alpha}{dT}\right) = \ln A + \ln(1 - \alpha) - \frac{E_a}{RT} \tag{16}$$

In peak temperature, $d\alpha/dT = 0$ and assume α is constant, yielding Eq. (17):

$$\ln\beta = \ln A + \ln(1 - \alpha p) - \frac{E_a}{RT_p} = \frac{-E_a}{R}\frac{1}{T_p} + \ln A + \ln(1 - \alpha p) \tag{17}$$

$$\ln(\beta) = -1.0516\frac{E_a}{RT_P} + \text{const.} \tag{18}$$

where β is the heating rate; T_p is the peak temperature; A is the pre-exponential factor; E_a is the activation energy; R is the gas constant. At the different heating rates, Ozawa's kinetic equation can be derived:

$$\ln\beta_1 + 1.0516\frac{E_a}{RT_{P_1}} = \ln\beta_2 + 1.0516\frac{E_a}{RT_{P_2}}$$

$$= \ln\beta_3 + 1.0516\frac{E_a}{RT_{P_3}} = ..., \tag{19}$$

Table 5
Results of safety parameters for TMCH 88 mass% with heating rates of 1, 2, 4, 6, and 8 °C/min.

Sample	TMCH 88 mass%				
Heating rate (°C/min)	1	2	4	6	8
T_{NR} (°C)	66	72	70	71	65
SADT (°C)	58	65	62	64	57

where β_1, β_2, and β_3 are the different heating rates; T_{P_1}, T_{P_2}, and T_{P_3} are the peak temperature of different heating rates. Results are displayed in Table 3 and Fig. 16.

3.2. Safety parameters evaluation

Safety parameters, such as T_{NR}, SADT, and TMR, are extensively used to evaluate the runaway reactions for reducing an unacceptable contingency by methodologies of Townsend and Fisher [15]. Evaluation methods of safety parameters were suitable for this study to evaluate the runaway reactions based on the experimental results. Both of the safety parameters are described as follows (Table 5).

3.2.1. Temperature of no return (T_{NR})

T_{NR} is an important index used to plan a suitable and deliverable emergency response measure, via evaluating the heat release rate and heat removal rate [16], and also extensively used to design a cooling system and to evaluate the remaining time for conducting a rescue operation [17]. Results by this study demonstrated that TMCH 88 mass% must be well controlled below 65 °C; it was the first discovered in the area of process safety. And, if the temperature is higher than 72 °C, a runaway reaction will be triggered in the next stage, in terms of TMCH 88 mass%. Because the TMCH 88 mass% plays an important role in polymerization as an initiator, therefore the thermal source should be removed from TMCH 88 mass% during the storage and transportation process. The following are the equations for T_{NR}.

$$(T_{NR} + 273.15)^2 = \frac{m \cdot E_a \Delta H \cdot k}{R \cdot U \cdot (1.8) \cdot a} \tag{20}$$

$$(T_{NR} + 273.15)^2 = \frac{m \cdot E_a \cdot \Delta H \cdot A \cdot e^{-E_a/R \cdot (T_{NR}+273.15)}}{R \cdot U \cdot (1.8) \cdot a} \tag{21}$$

3.2.2. Self-accelerating decomposition temperature (SADT)

SADT is defined as the lowest ambient air temperature at which a self-reactive substance of specified stability (contaminant level, inhibitor concentration, vessel volume filled ratio, etc.) undergoes an exothermic reaction in a specified commercial package in a period of 7 days or less [17]. A self-reactive substance [18,19] must be well temperature-controlled, have an inhibitor, and other ways for a container during transportation under SADT of less than or equal to 50 °C [4]. SADT of TMCH 88 mass% was obtained as about 57–65 °C, although it was higher than 50 °C, but it also needed a suitable controlled system for preventing an accident from occurring, because TMCH 88 mass% had a lower T_o ca. 106–126 °C and higher ΔH, more than 1300 kJ/kg. Eq. (22) was applied to calculate the SADT:

$$SADT = T_{NR} - \frac{R(T_{NR} + 273.15)^2}{E_a} \tag{22}$$

3.2.3. Time to maximum rate (TMR)

TMR was used to obtain the variation between time and temperature. We used four different isothermal conditions of 115, 120, 125, and 130 °C to compare each condition. According to the results, TMR was about 2.91–4.66 min in the higher temperature condi-

tions. The calculation method by Townsend and Tou [8] is shown in Eqs. (23) and (24):

$$TMR = \frac{RT^2}{AE_a \Delta T_{ad}} e^{-E_a/RT} \tag{23}$$

$$\Delta T_{ad} = \frac{Q}{C_p} \tag{24}$$

Experimental results were evaluated by nth order reaction with one exothermic peak; therefore, TMR could be precisely evaluated in this condition.

4. Conclusions

The effect of a runaway reaction of TMCH 88 mass% was evaluated using DSC. As the heating rate was set at lower rise condition, T_o was detected at lower temperature condition, because the decomposition reaction was in a more stable heat release range. ΔH was detected under isothermal and non-isothermal conditions, which also indicated that TMCH 88 mass% had a great quantity of heat during decomposition, due to its unstable structure of O–O having been interrupted. Theoretical analysis showed that an nth order reaction is the main way of thermal decomposition. However, the low value of E_a (122–140 kJ/mol) by calculation caused the normal atmospheric substance to decompose at high temperatures due to the runaway reaction for TMCH 88 mass%. The combination of the experimental analysis with theoretical calculations improved the understanding of the runaway reaction scenario of TMCH 88 mass%; this safety information could be employed by the petrifaction industry for preventing a hazard.

References

[1] A.S. Tompa, R.F. Boswell, Thermal stability of a plastic bonded explosive, Thermochim. Acta 357/358 (2000) 169–175.
[2] J. Yi, F. Zhao, S. Xu, L. Zhang, H. Gao, R. Hu, Effects of pressure and TEGDN content on decomposition reaction mechanism and kinetics of DB gun propellant containing the mixed ester of TEGDN and NG, J. Hazard. Mater. 165 (2009) 853–859.
[3] J.M. Tseng, C.M. Shu, J.P. Gupta, Y.F. Lin, Evaluation and modeling runaway reaction of methyl ethyl ketone peroxide mixed with nitric acid, Ind. Eng. Chem. Res. 46 (2007) 8738–8745.
[4] Safe Storage and Handling of Reactive Materials, Center for Chemical Process Safety of the AIChE, New York, USA, 1995, p. 226.
[5] S.Y. Cheng, J.M. Tseng, S.Y. Lin, J.P. Gupta, C.M. Shu, Runaway reaction on tert-butyl peroxybenzoate by DSC tests, J. Therm. Anal. Cal. 93 (2008) 121–126.
[6] Y.P. Chou, J.Y. Huang, J.M. Tseng, S.Y. Cheng, C.M. Shu, Reaction hazard analysis for the thermal decomposition of cumene hydroperoxide in the presence of sodium hydroxide, J. Therm. Anal. Cal. 93 (2008) 275–280.
[7] M.B. Talawar, R. Sivabalan, T. Mukundan, H. Muthurajan, A.K. Sikder, B.R. Gandhe, A. Subhananda Rao, Environmentally compatible next generation green energetic materials (GEMs), J. Hazard. Mater. 161 (2009) 589–607.
[8] D.M. Badgujar, M.B. Talawar, S.N. Asthana, P.P. Mahulikar, Advances in science and technology of modern energetic materials: an overview, J. Hazard. Mater. 151 (2008) 289–305.
[9] M.H. Keshavarz, Simple method for prediction of activation energies of the thermal decomposition of nitramines, J. Hazard. Mater. 162 (2009) 1557–1562.
[10] J.L. Martin, A. Cadenato, J.M. Salla, Comparative studies on the non-isothermal DSC curing kinetics of an unsaturated polyester resin using free radicals and empirical models, Thermochim. Acta 306 (1997) 115–126.
[11] H. Ma, B. Yan, Z. Li, Y. Guan, J. Song, K. Xu, R. Hu, Preparation, non-isothermal decomposition kinetics, heat capacity and adiabatic time-to-explosion of NTO·DNAZ, J. Hazard. Mater. 169 (2009) 1068–1073.
[12] C. Oommen, S.R. Jain, Ammonium nitrate: a promising rocket propellant oxidizer, J. Hazard. Mater. A67 (1999) 253–281.

[13] H.E. Kissinger, Reaction kinetics in differential thermal analysis, Anal. Chem. 29 (1957) 1702.
[14] T. Ozawa, Estimation of activation energy by isoconversion methods, Thermochim. Acta. 203 (1992) 159.
[15] D.I. Townsend, J.C. Tou, Thermochim. Acta 37 (1980) 1.
[16] H.G. Fisher, D.D. Goetz, J. Loss Prev. Process Ind. 6 (1993) 183.
[17] A.A. Kossoy, Y.G. Akhmetshin, Identification of kinetic models for the assessment of reaction hazards, Process Saf. Prog. 26 (3) (2007) 209.
[18] F. Sevim, F. Demir, M. Bilen, H. Okur, Korean J. Chem. Eng. 23 (2006) 736.
[19] Z. Hai, X. Zhiming, G. Pengjiang, H. Rongzu, G. Shengli, N. Binke, F. Yan, S. Qizhen, L. Rong, J. Hazard. Mater. 94 (2002) 205.